Cent. Eur. J. Chem. • 9(1) • 2011 • 25-34
DOI: 10.2478/s11532-010-0127-7

VERSITA

Central European Journal of **Chemistry**

Can lone pair-π and cation-π interactions coexist? A theoretical study.

Invited Paper

Carolina Estarellas*, Antonio Frontera*, David Quiñonero, Pere M. Deyà

Department of Chemistry, University of the Balearic Islands, 07122 Palma, Spain

Received 30 July 2010; Accepted 28 September 2010

Abstract: The interplay between two important noncovalent interactions involving different aromatic rings is studied by means of *ab initio* calculations (MP2/6-31++G**) computing the non-additivity energies. In this study we demonstrate the existence of cooperativity effects when cation−π and lone pair−π interactions coexist in the same system.

These effects are studied theoretically using energetic and geometric features of the complexes. In addition we use Bader's theory of atoms-in-molecules and Molecular Interaction Potential with polarization (MIPp) partition scheme to characterize the interactions. Experimental evidence for this combination of interactions has been obtained from the Cambridge Structural Database.

Keywords: *Noncovalent interactions • Cooperativity effects • Non-additivity energy • Atoms-in-Molecules theory • Energy partition scheme*

1. Introduction

Noncovalent interactions play a decisive role in many areas of modern chemistry. This is especially true in the field of supramolecular chemistry and molecular recognition, where the formation and function of supramolecular architectures occur through a variety of noncovalent forces. They are important in chemical reactions, molecular recognition and biological processes [1]. These chemical processes are accomplished with specificity and efficiency by means of intricate combinations of weak intermolecular interactions of various sorts. For this reason a deep understanding and quantification of intermolecular interactions is important for the rationalization of effects observed in several fields, such as biochemistry and materials science. A quantitative description of these interactions can be obtained by taking advantage of quantum chemical calculations on small model systems [2-4]. In complex biological systems and in the solid state a multitude of these noncovalent interactions may operate simultaneously, giving rise to interesting cooperativity effects. In particular, interactions involving aromatic rings are often key binding forces in both chemical and biological systems [1]. For instance, cation–π interactions [5-10] are supposed to be an important factor to the ammonia transporter proteins [11]. They are also important for the binding of acetylcholine to the active site of the enzyme acetylcholine esterase [12], and, recently, their importance has been demonstrated in neurotransmitter receptors [13]. The cation–π interaction is dominated by electrostatic and ion-induced polarization terms [14]. The nature of the electrostatic term can be rationalized in terms of the permanent quadrupole moment of the arene. For around eight years, a new type of supramolecular interaction, namely anion–π interaction [15-17] has been increasingly reported in the literature. Egli and co-workers have extended this concept to a more general form, namely lone pair–π interaction (lp–π) [18]. They reported two clear cases of lp–π interactions in biomacromolecules: (a) the stabilization of the structure of *Z*-DNA [19,20] and (b) H_2O-π interactions within a ribosomal frame-shifting RNA pseudoknot [21]. Indeed, lp–π interactions have been found to be of great importance for the stabilization of biological macromolecules, as well as for the binding of inhibitors in the binding pocket of biochemical receptors [22]. Very recently, in a comprehensive review [23], Gamez *et al.* designated such lp–π contacts as a new supramolecular bond and a rigorous analysis of the Cambridge Structure Database (CSD) revealed that

* *E-mail: toni.frontera@uib.es*
carol.estarellas@uib.es

such contacts are not unusual in organic/coordination compounds but have been overlooked in the past. This thorough survey of the CSD clearly shows that lp–π interactions are actually ubiquitous in solid-state structures. Surprisingly, only a few examples of lp–π interactions involving small synthetic molecules have been reported; this topic has scarcely been studied [24-27]. Therefore, current research investigations are aimed at systematically studying this type of noncovalent bonding interaction observed in new crystal structures, to gain knowledge in this nascent field, both theoretically and experimentally.

In this work, we study how the cation–π influences the lp–π interaction and *vice versa* in complexes where both interactions are present. It has been demonstrated that both interactions are very important in biological systems. Therefore, it is interesting to study the interplay between them. We have selected three aromatic rings, see Fig. 1, that contain different numbers of fluorine substituents in their structure (benzene, **A**; trifluorobenzene, **B** and hexafluorobenzene, **C**). These allow us to study the strength of both interactions depending on the electrostatic nature of the π cloud. We have selected Na^+ and Mg^{2+} cations to perform this study in order to analyze how these effects are influenced by the charge and size of the cation. We have chosen two molecules, water and ammonia, to study the lone pair-π interaction. We have selected water as the model for oxygen as the lone pair donating group and ammonia as the model for nitrogen as the lone pair donating group. For every aromatic ring, we have calculated the cation–π (**1A**-**C** and **2A**-**C**) and lone pair–π binary complexes, (**3A**-**C** and **4A**-**C**) (see Fig. 2), and cation-π-lp ternary complexes (see Fig. 3). We have used the Bader's theory of "atoms-in-molecules" (AIM) [28], which has been widely used to characterize a great variety of interactions and in particular cation–π and lp–π interactions [29,30], to analyze cooperative effects in the complexes. We have used the Molecular Interaction Potential with polarization partition scheme [31] to investigate the physical nature of the interplay between the two types of interaction.

2. Theoretical Methods

The geometries of all complexes studied in this work were optimized at the MP2/6-31++G** level of theory. These calculations have been carried out within the Gaussian-03 package [32]. The binding energies were calculated with correction for the basis set superposition error (BSSE) by using the Boys-Bernardi counterpoise

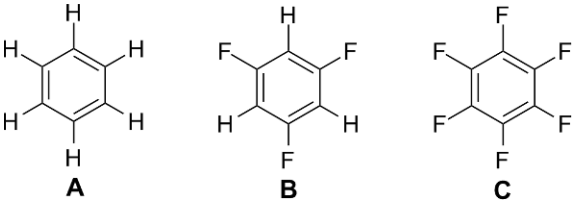

Figure 1. Aromatic compounds **A-C**.

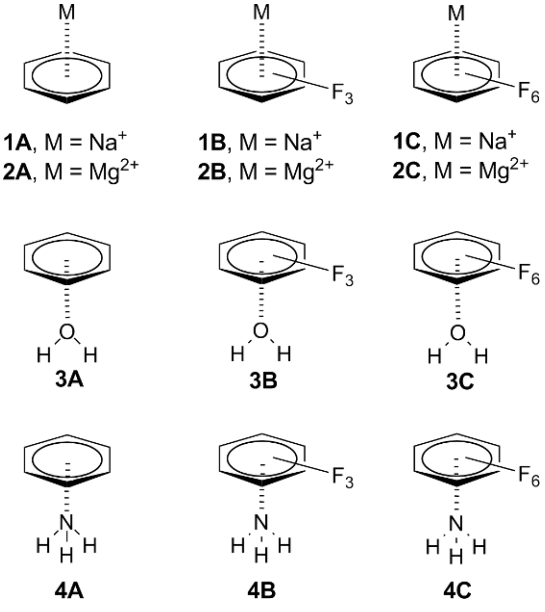

Figure 2. Cation-π complexes **1A-C** and **2A-C** and lone pair-π complexes **3A-C** and **4A-C**.

technique [33]. The optimization of the molecular geometries has been performed imposing the highest symmetry point group.

In complexes where lone pair–π and cation–π interactions coexist, we have computed the genuine non-additivity energies (E-E_A) using Eq. 1. Thus the non-additivity energies are computed by subtracting the binding energy of the sum of all pair interaction energies (E_A) from the binding energy of the complex (E).

$$E\text{-}E_A = E_{abc} - (E_{ab} + E_{ac} + E_{bc}) \quad (1)$$

The AIM analysis has been performed by means of the AIM2000 version 2.0 program [34] using the MP2/6-31++G** wave function. We have evaluated the charge transfer in the complexes by using the Merz-Kollman (MK) scheme for deriving atomic charges at the MP2/6-31++G** level of theory. It has been reported that this method provides high quality charges [35].

The physical nature of the noncovalent interactions has been studied using Molecular Interaction Potential with polarization (MIPp) [31] method using the HF/6-31++G**//MP2/6-31++G** wave function by means of

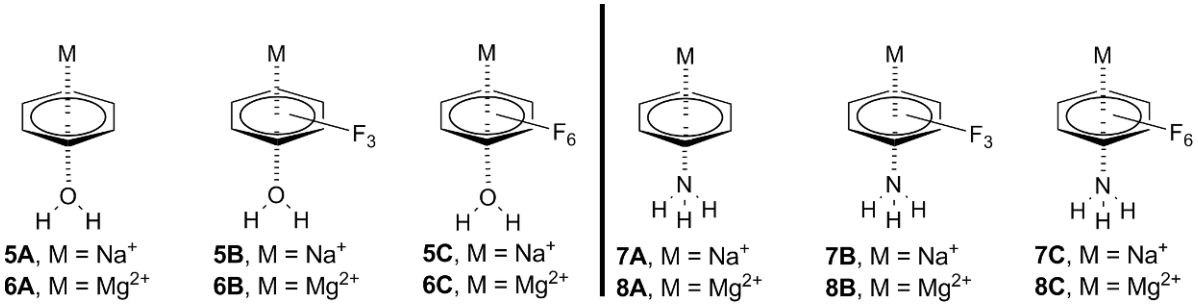

Figure 3. Left: Water ternary complexes **5A-C** and **6A-C**. Right: Ammonia ternary complexes **7A-C** and **8A-C**.

the MOPETE-98 program [36]. The MIPp is a convenient tool for predicting binding properties. It has been successfully used for rationalizing molecular interactions such as ion–π interactions and for predicting molecular reactivity [37,38]. The MIPp partition scheme is an improved generalization of the MEP where three terms contribute to the interaction energy, (i) an electrostatic term identical to the MEP [39], (ii) a classical dispersion–repulsion term [40], and (iii) a polarization term derived from perturbational theory [41]. The Na^+ cation was considered as a classical interacting particle and the van der Waals parameters were taken from the literature [42].

3. Results and Discussion

3.1. Preliminary results

In the following sections of the paper we will use the value of the density at some critical points that characterize the different noncovalent interactions to study the interplay between them. It has been proposed that the density at the critical points can be used as a measure of bond order [17,43]. Therefore the variation of these values in a system where several interactions coexist (ternary system) in comparison with one where only one interaction is present (binary system) gives information about the strengthening/weakening of the interactions. In Fig. 4 we show the distribution of critical points (CP) in several complexes to visualize the CPs that characterize each type of interaction. For cation–π complexes **2A** and **2C** we found six bond CP (red spheres), six ring CP (yellow spheres) and one cage CP (green sphere). In complex **2B** the interaction is characterized by three bond, three ring and one cage CP. Lone pair–π complexes are represented by **3A** for the water molecule and by **4A** for the ammonia molecule. In complex **3A** we found two bond, two ring and one cage CPs connecting the oxygen atom with the aromatic ring. In complex **4A** the interaction is characterized by three bond, three ring and one cage CPs. In Fig. 4 we show the distribution of CPs for the ternary complexes **6A** and **8A**. For all ternary complexes, the cation–π interaction is characterized by six bond, six ring and one cage CPs. Conversely, the distribution of CPs that characterizes the lp–π interaction depends on the lone pair donor molecule. For **6A** (H_2O) we found two bond, two ring and one cage CPs, and for **8A** (NH_3) we found six bond, six ring and one cage CPs.

Table 1. Interaction energies without and with the BSSE (ΔE and ΔE_{BSSE}, respectively in kcal mol^{-1}), equilibrium distances ($R_{C\pi}$, Å), the computed Merz-Kollman charges of the cation (Q_{MK}) and the density at the cage critical point (ρ, a.u.) at the MP2/6-31++G** level of theory.

Compound	ΔE	ΔE_{BSSE}	$R_{C\pi}$	Q_{MK}	$10^2\rho_{C\pi}$
1A	-24.75	-21.12	2.424	0.76	0.8122
1B	-10.24	-7.89	2.570	0.81	0.6639
1C	1.01	2.70	2.836	0.85	0.4345
2A	-114.79	-108.82	1.963	1.29	1.8284
2B	-81.56	-77.11	2.038	1.40	1.7326
2C	-53.27	-48.71	2.112	1.40	1.5540

3.2. Energetic and geometric results

In Table 1, we summarize the binding energies without and with the basis set superposition error (BSSE) correction (ΔE and ΔE_{BSSE}, respectively) and equilibrium distances ($R_{C\pi}$) for the cation–π complexes **1A-C** and **2A-C** (see Fig. 2) at the MP2/6-31++G** level of theory. From inspection of the results several interesting points emerge. As expected, when the aromatic ring is electron-rich, the cation–π interaction is more favorable. On the other hand, it is interesting to note that, regardless of the aromatic ring, the interaction becomes more favorable when the cation is divalent. This fact is striking because the interaction between electron-deficient aromatic rings and cations is electrostatically unfavorable. We could anticipate that the repulsion involving the quadrupole moment of hexafluorobenzene (Q_{zz} = +9.50 B) and the cation should increase from monovalent to divalent cations, in clear disagreement with the interaction energies computed for **1C** and **2C**. A previously reported study on the binding nature of the M^{2+}-π interaction [44] helps us to find a likely explanation about the features observed in Table 1. They propose that the interaction between alkaline earth metal cations

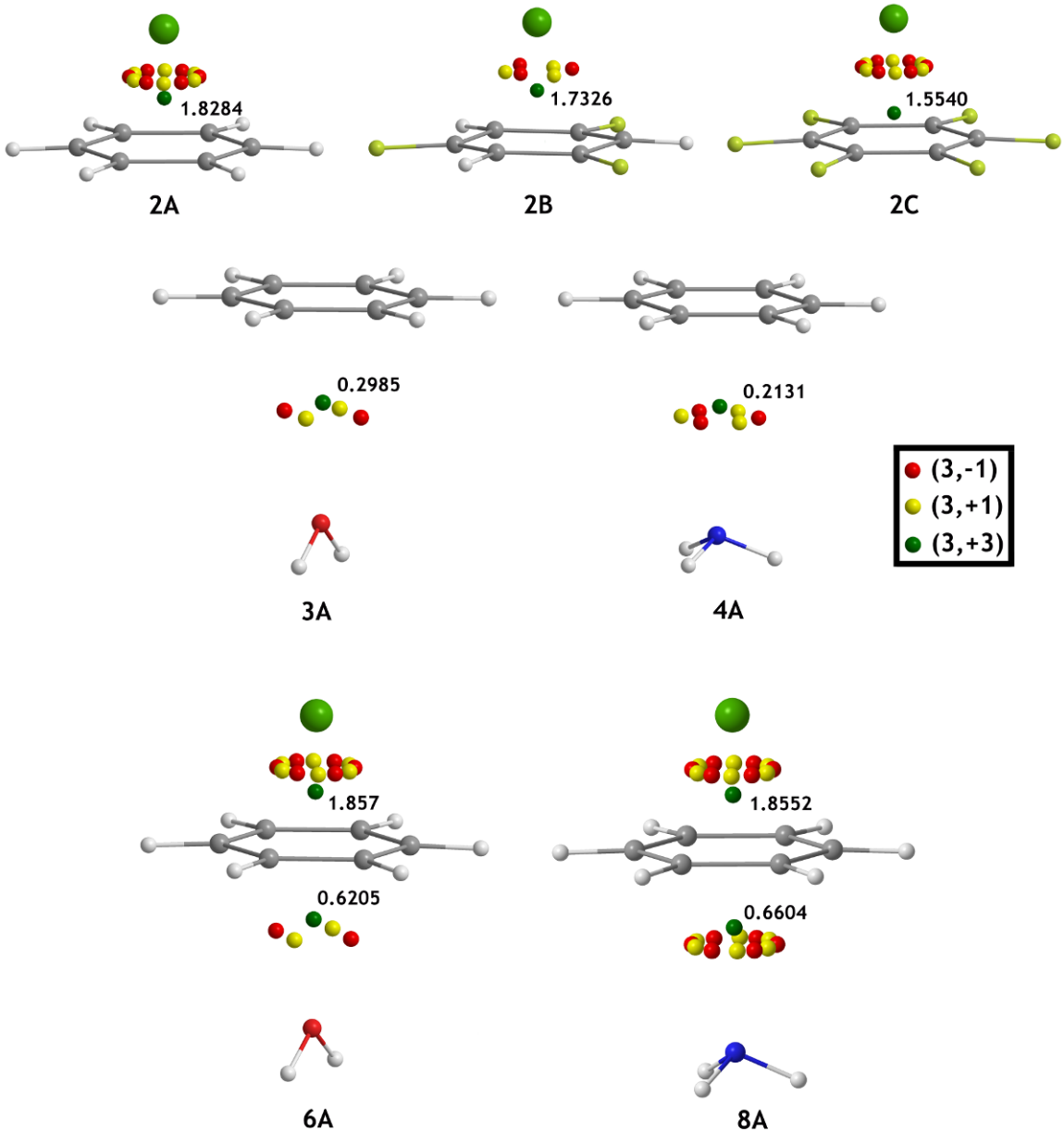

Figure 4. Distribution of critical points for cation–π (**2A-C**), lone pair–π (**3A** and **4A**) and ternary complexes (**6A** and **8A**).

and benzene is so strong that it should be considered a chemical bond rather than the usual molecular interaction. This suggestion implies that this interaction might be different in nature from the interaction between monovalent cations and aromatic rings. In addition, they demonstrate that the interaction between substituted benzenes and Mg^{2+} has the nature of a chemical bond. In fact, distances between divalent cations and aromatic rings are even shorter than the covalent bond length between carbon and the corresponding metal. This different binding mode of divalent cations can explain the very different energetic results obtained for **1C** and **2C**. From the geometrical point of view we emphasize two remarkable points. For the same cation, as we move from **A** to **C** aromatic rings the distances increase, *i.e.,* for complex **1A** (Na^++benzene) the equilibrium distance is 2.424 Å, while for complex **1C** (Na^++hexafluorobenzene) the distance of interaction is 2.836 Å. For the same aromatic ring, increasing the charge of the cation, the distances of the complex are smaller. For instance, for complex **1A** (Na^++benzene) the equilibrium distance is 2.424 Å, while for complex **2A** (Mg^{2+}+benzene) the

distance of interaction is 1.963 Å. The small equilibrium distances observed for magnesium complexes are an indication of partially covalent interaction between the divalent cation and aromatic rings. In Table 1 we include the charge of the cation in the complex to study the charge transfer effects. For the complexes **1A**-**C**, we observe that in complex **1A** the charge transfer is greater and decreases as we move from **A** to **C**. This is in agreement with energetic and geometric results. For complexes **2A**-**C** the trend is similar. The values of ρ at the cage CPs are also included in Table 1. For complexes **1A-C** we observe that the charge density decreases as the π acidity of the ring increases. Thus, we can use it to measure the strengthening or weakening of the interaction. This result is in agreement with the variation of equilibrium distances and charge transfer. The same is observed for complexes **2A-C.** We have found an interesting relationship between charge density (ρ) at the cage critical point and the binding energies with BSSE correction (ΔE_{MP2}) (see Fig. 5). For cation–π complexes we have obtained a regression coefficient R = 0.948, confirming that the values of ρ at the cage CP are a good measure of bond order [29].

Briefly, for cation–π complexes, the strength of the interaction strongly depends upon the nature of the ring and the charge of the cation. The most important point is the surprising behavior of magnesium cation interacting with the electron deficient aromatic ring.

The geometric and energetic results computed for lone pair–π complexes **3A-C** and **4A-C** (see Fig. 2) are summarized in Table 2. Some very interesting points can be extracted from the results. The energetic and geometric features of lp–π complexes **3A-C** indicate that the interaction is more favorable as the π acidity of the ring increases. For example, the interaction between water and benzene in complex **3A** presents a positive interaction energy of 1.14 kcal mol^{-1}, while the interaction with hexafluorobenzene in complex **3C** presents a negative interaction energy of -3.08 kcal mol^{-1} (BSSE corrected). The same trend is observed for complexes **4A-C**. This fact is in agreement with geometric results, since as the interaction energy of the complex becomes more favorable the equilibrium distance decreases. We have also found an excellent relationship between the charge density (ρ) at the cage critical point and the binding energies with BSSE correction (ΔE_{MP2}). For lp–π complexes we have obtained a regression coefficient of R = 0.955 (see Fig. 6), indicating that the values of ρ are a good quality measure of bond order. The charge density is larger in complexes where the lone pair–π interaction is more favorable. For the same aromatic ring, there is little difference between water and ammonia as interacting lone pair donor molecules. The energetic,

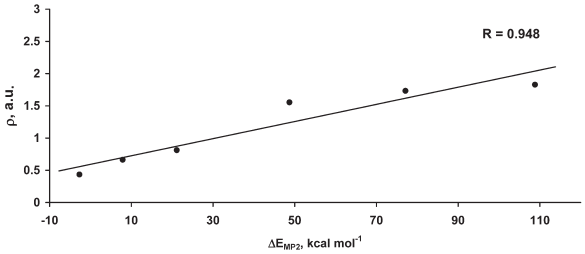

Figure 5. Regression plot between the variation of the charge density (ρ) at the cage critical point and binding energies (ΔE_{MP2}) of cation–π complexes **1A-C** and **2A-C**.

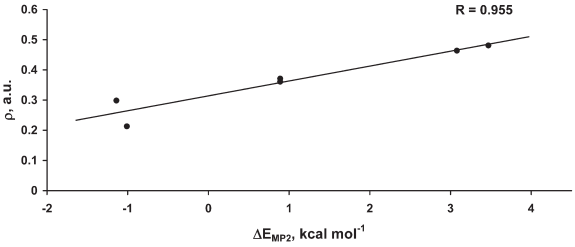

Figure 6. Regression plot between the variation of the charge density (ρ) at cage critical point and binding energies (ΔE_{MP2}) of lp–π complexes **3A-C** and **4A-C**.

Table 2. Interaction energies without and with the BSSE (ΔE and ΔE_{BSSE}, respectively in kcal mol^{-1}), equilibrium distances ($R_{lp\pi}$, Å) and the density at the cage critical point (ρ, a.u.) at the MP2/6-31++G** level of theory.

Compound	ΔE	ΔE_{BSSE}	$R_{lp\pi}$	$10^2\rho_{lp\pi}$
3A	-0.23	1.14	3.426	0.2985
3B	-2.55	-0.89	3.183	0.3610
3C	-5.04	-3.08	3.006	0.4639
4A	-0.27	1.01	3.724	0.2131
4B	-2.64	-0.89	3.370	0.3712
4C	-5.76	-3.47	3.193	0.4810

geometric and topological results indicate that the lp–π interaction is similar for water and ammonia. This is probably due to a compensating effect. Ammonia has only one lone pair available for interacting with the ring, whilst water has two. However, the lone pair of ammonia is pointing directly to the center of the ring.

In brief, the lone pair–π interaction is more favorable with electron-deficient aromatic rings, as expected. Curiously the strength of the interaction is analogous for water and ammonia complexes.

In order to further investigate the mutual influence of the interactions we have computed the energies of the ternary complexes shown in Fig. 3. We have calculated the interaction and non-additivity energies with BSSE correction (see Table 3). We observe that in all cases the interaction energy is favorable, since in the ternary complexes the cation-π interaction is energetically dominant. The most favorable complexes correspond to benzene. For instance, complex **5A** (Na^++**A**+H_2O) is ~20 kcal mol^{-1} more favorable than **5C** (Na^++**C**+H_2O).

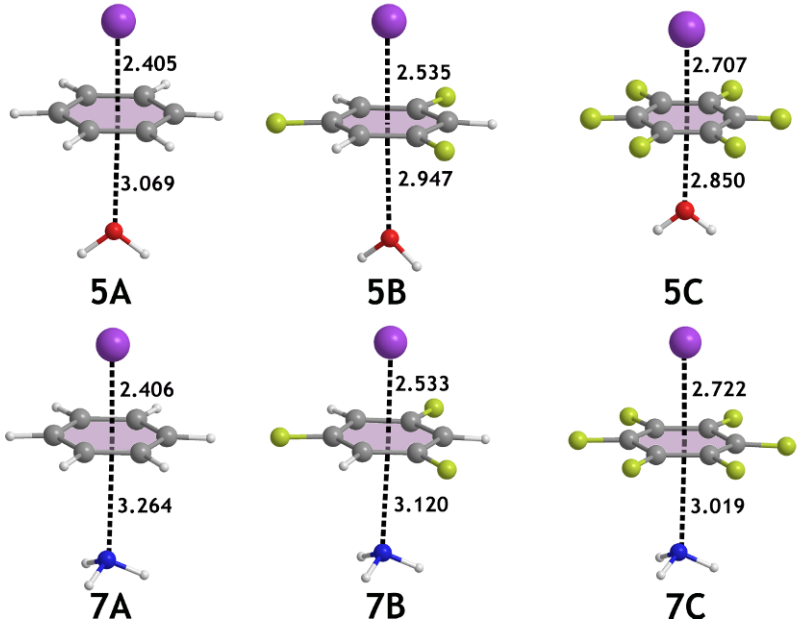

Figure 7. Optimized ternary complexes **5A-C** and **7A-C**.

Table 3. Interaction and non-additivity energies with the BSSE (ΔE_{BSSE} and $E\text{-}E_A$, kcal mol^{-1}), equilibrium distances ($R_{C\pi}$, $R_{lp\pi}$, Å), the computed Merz-Kollman charges of the cation (Q_{MK}) and the density at the cage critical point (**ρ**, a.u.) at the MP2/6-31++G** level of theory. The variation of the equilibrium distance (ΔR) and charge density ($\Delta\rho$) at the cage CP of the complexes with respect to complexes **1A-C** and **2A-C** (Cπ) and **3A-C** and **4A-C** (lp–π) is also summarized. (Legend, Cπ = cation–π, lp-π = lone pair–π).

Compound	ΔE_{BSSE}	$E\text{-}E_A$	$R_{C\pi}$	$R_{lp\pi}$	$\Delta R_{C\pi}$	$\Delta R_{lp\pi}$	Q_{MK}	$10^2\rho_{C\pi}$	$10^2\rho_{lp\pi}$	$10^3\Delta\rho_{C\pi}$	$10^3\Delta\rho_{lp\pi}$
5A	-25.58	-1.27	2.405	3.069	-0.019	-0.357	0.835	0.8455	0.4143	0.333	1.158
5B	-14.64	-2.02	2.535	2.947	-0.035	-0.236	0.851	0.7112	0.5027	0.473	1.417
5C	-5.61	-1.96	2.707	2.850	-0.129	-0.156	0.850	0.5490	0.5612	1.145	0.973
6A	-122.84	-4.16	1.951	2.783	-0.012	-0.643	1.544	1.8570	0.6205	0.286	3.220
6B	-94.11	-8.73	2.025	2.708	-0.013	-0.475	1.602	1.7603	0.7039	0.277	3.429
6C	-68.31	-9.92	2.099	2.647	-0.013	-0.359	1.590	1.5634	0.7452	0.094	2.813
7A	-25.22	-1.24	2.406	3.264	-0.018	-0.460	0.872	0.8461	0.5100	0.339	2.969
7B	-14.52	-2.12	2.533	3.120	-0.037	-0.250	0.886	0.7172	0.5193	0.533	1.481
7C	-6.14	-1.96	2.722	3.019	-0.114	-0.174	0.909	0.5442	0.5884	1.097	1.074
8A	-123.25	-0.58	1.955	2.935	-0.008	-0.789	1.642	1.8552	0.6604	0.268	4.473
8B	-95.22	-5.62	2.031	2.846	-0.007	-0.524	1.649	1.7573	0.7632	0.247	3.920
8C	-70.16	-7.34	2.110	2.778	-0.002	-0.415	1.674	1.5619	0.8100	0.079	3.290

When we compare the results for sodium complexes, depending on the lone pair donor molecule **5A-C** (H_2O) and **7A-C** (NH_3), see Fig. 7, we observe that the binding energies are almost the same. A similar situation is observed for complexes **6A-C** and **8A-C**. As previously observed for binary complexes, the binding energies are insensitive to the lone pair donor molecule. To study if cooperativity effects exist we analyze non-additivity energies and equilibrium distances. Non-additivity energies ($E\text{-}E_A$) are negative in all complexes. This means that there is a favorable cooperative effect between cation–π and lp–π interactions. Examining the results we observe that the most stable complex (**8A**) presents the smallest cooperativity effect (smaller $E\text{-}E_A$). This fact is repeated in every complex series (**A-C**). The stability of a complex is measured using the complexation energy, which is directly proportional to the strength of the noncovalent interactions that are involved in the formation of the complex. We have recently reported theoretical [45] evidences that in ternary complexes, the most stable usually implies a very modest weakening or strengthening of the noncovalent interactions in comparison to the binary complexes. This fact is clearly shown for each series of magnesium cation complexes. The most energetically stable complexes have the smallest non-additivity energies (**A** complexes).

Concerning the geometric features, if we analyze $\Delta R_{C\pi}$ and $\Delta R_{lp\pi}$ in Table 3 all the distances shorten. The $\Delta R_{C\pi}$ values are larger in sodium complexes than in magnesium complexes. This is because the cation–π equilibrium distances of complexes **2A-C** (see Table 1) are initially very short (partially covalent

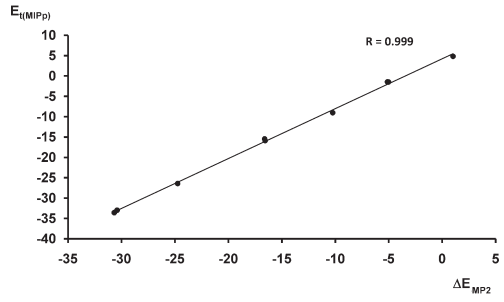

Figure 8. Regression plot between the variation of the total energy contribution in MIPp of **A-C**, **3A-C** and **4A-C** binary systems and interaction energies (ΔE_{MP2}) of the ternary complexes **1A-C**, **5A-C** and **7A-C**.

bond) thus limiting scope for further reductions. The $\Delta R_{Ip\pi}$ values are larger in magnesium complexes. This can be attributed to the binding force of the cation–π which is greater in these complexes, a fact that simultaneously provokes a reinforcement of the Ip–π interaction. The AIM analysis gives some helpful information regarding the strength of the noncovalent interactions involved in the complexes. In Fig. 4, we show the distribution of CPs for several complexes. In Table 3, we gather the values of the electron charge density (ρ) computed at the cage CP that characterizes cation–π and Ip–π interactions and we summarize the variation of these values ($\Delta\rho$) with respect to **1A-C** and **2A-C** for cation–π and **3A-C** and **4A-C** for Ip–π. These values give information about the interplay between noncovalent interactions

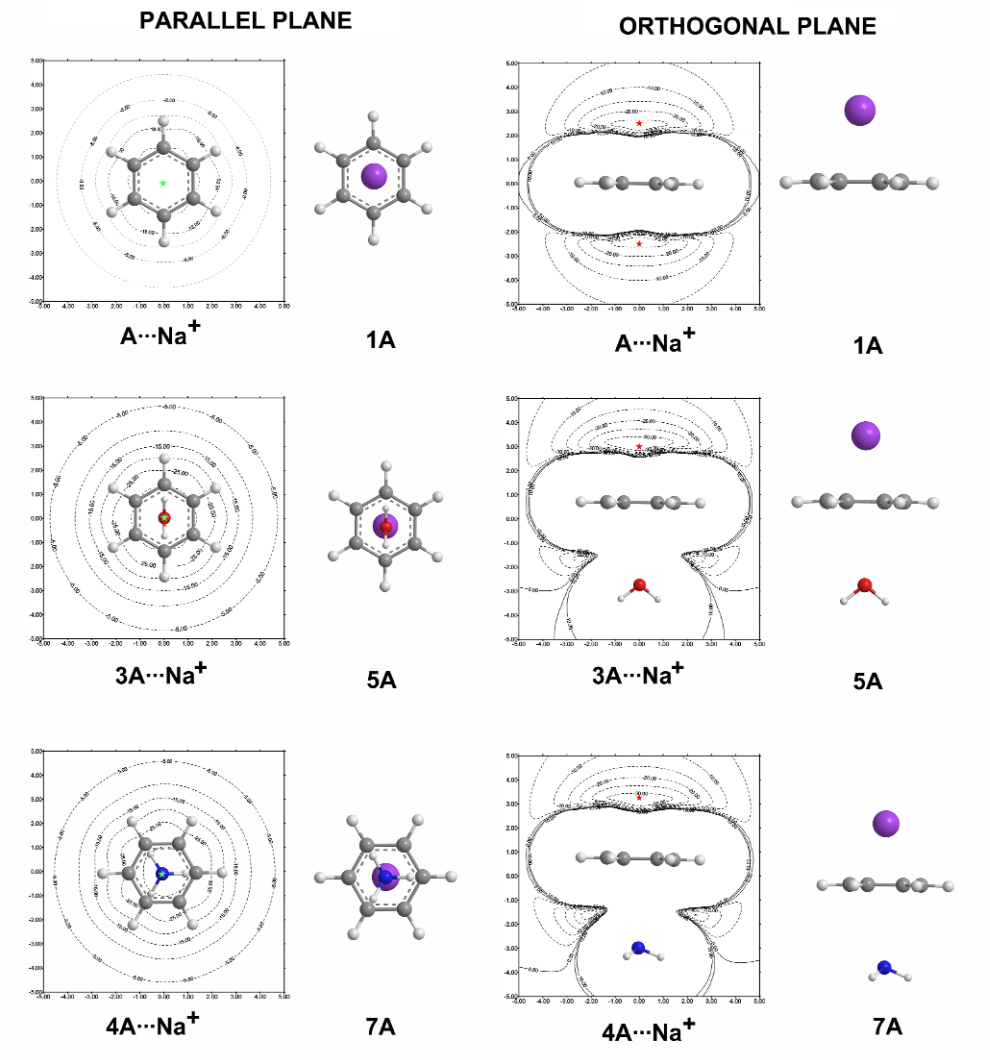

Figure 9. Left: 2D-MIPp(Na^+) energy maps computed for **A**, **3A** and **4A** above the molecular plane. Contour lines are plotted every 5 kcal mol^{-1}. The minimum energy is symbolized by a green star. Axis units are Å, and energies are in kcal mol^{-1}. Right: 2D-MIPp(Na^+) energy maps computed for **A**, **3A** and **4A** at the orthogonal plane. Contour lines are plotted every 5 kcal mol^{-1}. The minimum energy is symbolized by a red star. On the right of 2D-MIPp energy maps the plan views (above molecular plane) and front views (at orthogonal plane) of the optimized **1A**, **5A** and **7A** complexes are represented.

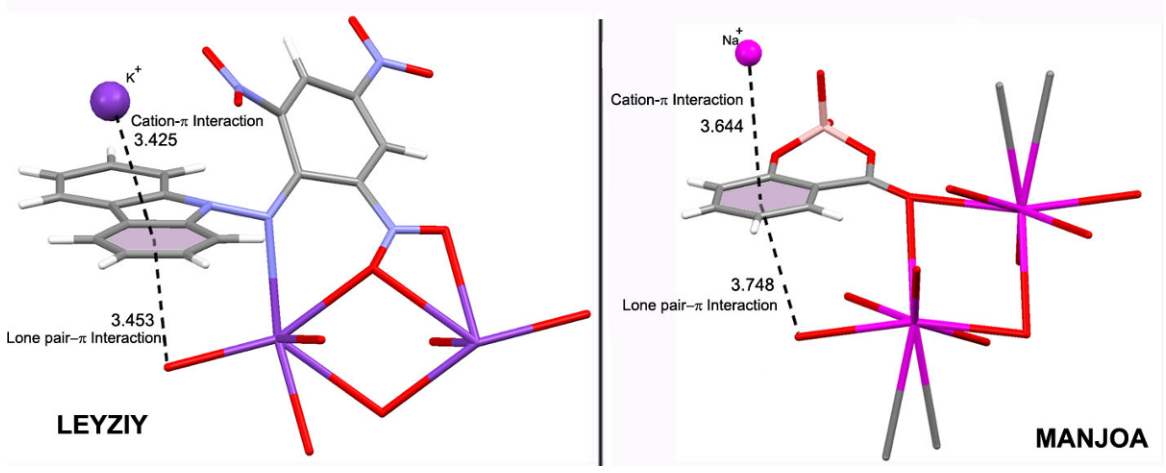

Figure 10. Partial views of the X-ray structures exhibiting combination of two noncovalent interactions. The CSD codes are shown. Distances in Å.

involved in the complexes. It is worth mentioning that the value of the charge density computed at the cage CPs is greater in ternary complexes (see Fig. 3) than in binary complexes (see Fig. 2). Finally, in Table 3, we also include the charge of the cation in the complexes in order to study the charge transfer effects. It can be observed that in all complexes the charge transfer is important, especially in magnesium complexes (**6A-C** and **8A-C)**, probably because of the shorter equilibrium distance of the cation–π complexes. We conclude that in the ternary complexes the interplay between both interactions is favorable, as demonstrated by energetic and geometric parameters and AIM results.

3.3 MIPp Analysis

We have used MIPp partition scheme to analyze the physical nature of the cation–π interaction involved in the complexes and to understand the bonding mechanism and the non-additivity effects. We have computed the MIPp of compounds **A-C, 3A-C** and **4A-C** interacting with Na^+ to analyze the cation–π interaction in the absence (**A-C**) and presence (**3A-C** and **4A-C**) of lone pair–π interactions (see Table 4). A good agreement between the MIPp energies and the computed interaction energies of the complexes at MP2/6-31++G** can be observed. These interaction energies have been computed considering ternary complexes as binary systems, where the dimers have been previously formed. That is to say, we have computed **5A** (ternary complex) interaction energy as result of the sum of interaction energies of complex **3A** and Na^+, (**5A** = **3A** + Na^+). The agreement between the MP2 and MIPp energies indicates the reliability of the MIPp partition scheme. In fact, comparison of the two sets of values gives a linear regression plot with a coefficient R = 0.999 as shown in Fig. 8.

In all cases the polarization (E_{pol}) contribution is large and negative and independent of the π acidity of the ring. The total interaction energy (E_t) computed using MIPp becomes less favorable when the aromatic ring changes from electron-rich (**A)** to electron-deficient **(C)**. The MIPp interaction energy decreases on going from complex **A**···Na^+ to **C**···Na^+ which is basically due to electrostatic effects. The polarization term varies slightly from **A** to **C** compounds and the electrostatic term clearly becomes more positive as the π acidity of the aromatic ring increases. From the energetic results of Table 4 we can deduce that the cooperativity effects are mainly due to the electrostatic contribution. For instance, the E_e term in complex **3A**···Na^+ is more negative (6 kcal mol^{-1}) than the one computed for complex **A**···Na^+. In contrast the E_{pol} and E_{vw} terms are very similar, with variations of less than 1 kcal mol^{-1}. Similar behavior is observed for the rest of complexes. In Fig. 9 we represent the bidimensional MIPp (2D-MIPp) maps obtained for **A**, **3A** and **4A** interacting with Na^+. We have computed two 2D-MIPp maps, one orthogonal and the other parallel to the molecular plane to study the cation-binding ability of **A** (benzene), **3A** (benzene+H_2O), **4A** (benzene+NH_3). An excellent agreement can be observed between the location of the minima in 2D-MIPp energy maps and the geometry of the optimized complexes.

3.4. CSD Analysis

To obtain experimental evidence of the coexistence of two interactions we performed a search in the Cambridge Structural Database (CSD) [46]. Crystal structures are so rich in geometrical information and often reveal effects that have not been noticed by the original authors. The utility of crystallography and the CSD in analyzing geometrical parameters and noncovalent interactions is clearly established [47]. In exploring the CSD we found

Table 4. Electrostatic (E_e), polarization (E_{pol}) and van der Waals (E_{vw}) contributions to the total (E_t) interaction energy (kcal mol^{-1}) computed using MIPp for **A-C**, **3A-C** and **4A-C** interacting with Na^+ at equilibrium distances from the aromatic ring.

Compound	E_e	E_{pol}	E_{vw}	E_t	ΔE_{MP2}
A···Na^+	-15.58	-15.43	4.59	-26.43	-24.75
B···Na^+	1.93	-12.27	1.29	-9.05	-10.24
C···Na^+	14.45	-9.58	-0.07	4.79	1.01
3A···Na^+	-21.41	-16.32	4.15	-33.59	-30.68[a]
3B···Na^+	-4.22	-15.00	3.30	-15.91	-16.56[a]
3C···Na^+	8.68	-10.17	0.01	-1.48	-5.03[a]
4A···Na^+	-21.23	-17.41	5.67	-32.98	-30.41[a]
4B···Na^+	-3.84	-15.45	3.80	-15.48	-16.6[a]
4C···Na^+	9.63	-11.82	0.72	-1.47	-5.12[a]

[a]*Computed as binary complexes (**3A-C** + Na^+, **4A-C** + Na^+)*

several structures in which noncovalent π interactions are present among alkaline cations, aromatic rings and atoms such N, O, S, F, Cl, Br and I bearing a lone pair electron. Two selected examples retrieved from CSD (codes LEYZIY [48] and MANJOA [49]) are shown in Fig. 10, in which the cation–π and lp–π interactions are evident and play a prominent role in the crystal packing. In LEYZIY structure the potassium cation establishes one cation–π interaction with a phenyl ring of the carbazole group. In addition, the same aromatic ring establishes a lone pair–π interaction with an oxygen atom that is bonded to other potassium cation. In the MANJOA structure the cation interacts with a salicylic acid motif, which at the same time interacts with an oxygen atom at the opposite side of the aromatic ring. The equilibrium distances observed in the solid state are larger than the theoretical ones because the cation and molecules that participate in the lp–π establish other noncovalent interactions, which are not shown for the sake of clarity.

4. Conclusions

The results reported in this manuscript stress the importance of the interplay between noncovalent interactions involving different aromatic systems that can lead to synergistic stability. These effects have been studied using genuine non-additivity energies and the Bader's AIM theory. The MIPp partition scheme demonstrates that the cooperativity effects mainly result from the electrostatic term. Due to the presence of a great number of lone pair–π and cation–π interactions in biological systems, these effects can be important and might help to understand some biological processes where interplay between many interactions may exist. We have also found that the cation–π interaction can be enhanced as a consequence of the simultaneous participation of the lone pair–π interaction especially with electron-deficient aromatic rings.

Acknowledgements

C.E. thanks the MEC of Spain for a fellowship. D. Q. thanks to MICINN of Spain for "Ramon y Cajal Contract". We thank the MICINN of Spain (project CTQ2008-00841/BQU) for financial support. We thank the Centre de Supercomputació de Catalunya (CESCA) for computational facilities.

References

[1] E.A. Meyer, R.K. Castellano, F. Diederich, Angew. Chem. Int. Ed. 42, 1210 (2003)
[2] A.K. Rappé, E.R. Bernstein, J. Phys. Chem. A 104, 6117 (2000)
[3] A. Hesselmann, G. Jansen, M. Schütz, J. Am. Chem. Soc. 128, 11730 (2006)
[4] M. Piacenza, S. Grimme, Chem. Phys. Chem. 6, 1554 (2005)
[5] J.C. Ma, D.A. Dougherty, Chem. Rev. 97, 1303 (1997)
[6] J.P. Gallivan, D.A. Dougherty, Proc. Natl. Acad. Sci. USA 96, 9459 (1999)
[7] G.W. Gokel, S.L.D. Wall, E.S. Meadows, Eur. J. Org. Chem. 2967 (2000)
[8] G.W. Gokel, L.J. Barbour, S.L.D. Wall, E.S. Meadows, Coord. Chem. Rev. 222, 127 (2001)
[9] G.W. Gokel, L.J. Barbour, R. Ferdani, J. Hu, Acc. Chem. Res. 35, 878 (2002)
[10] C.A. Hunter, J. Singh, J.M. Thorton, J. Mol. Biol. 218, 837 (1991)
[11] H. Ishikita, E.W. Knapp, J. Am. Chem. Soc. 129, 1210 (2007)
[12] D.A. Dougherty, Science 271, 163 (1996)
[13] S.C.R. Lummis, D.L. Beene, N.J. Harrison, H.A. Lester, D.A. Dougherty, Chem. Biol. 12, 993 (2005)
[14] E. Cubero, F.J. Luque, M. Orozco, Proc. Natl. Acad. Sci. USA 95, 5976 (1998)
[15] M. Mascal, A. Armstrong, M.D. Bartberger, J. Am. Chem. Soc. 124, 6274 (2002)
[16] I. Alkorta, I. Rozas, J. Elguero, J. Am. Chem. Soc. 124, 8593 (2002)
[17] D. Quiñonero, C. Garau, C. Rotger, A. Frontera, P. Ballester, A. Costa, P.M. Deyà, Angew. Chem. Int. Ed. 41, 3389 (2002)
[18] M. Egli, S. Sarkhel, Acc. Chem. Res. 40, 197 (2007)

[19] M. Egli, R.V. Gessner, Proc. Natl. Acad. Sci. U.S.A. 92, 180 (1995)
[20] D. Bancroft, L.D. Williams, A. Rich, M. Egli, Biochemistry 33, 1073 (1994)
[21] S. Sarkhel, A. Rich, M. Egli, J. Am. Chem. Soc. 125, 8998 (2003)
[22] J.C. Calabrese, D.B. Jordan, A. Boodhoo, S. Sariaslani, T. Vannelli, Biochemistry, 43, 11403 (2004)
[23] T.J. Mooibroek, P. Gamez, J. Reedijk, CrystEngComm 10,1501 (2008)
[24] P. de Hoog, A. Robertazzi, I. Mutikainen, U. Turpeinen, P. Gamez, J. Reedijk, Eur. J. Inorg. Chem. 2684 (2009)
[25] P.J. Kitson, Y.F. Song, P. Gamez, P. de Hoog, D.L. Long, A.D.C. Parenty, J. Reedijk, L. Cronin, Inorg. Chem. 47, 1883 (2008)
[26] Z.L. Lu, P. Gamez, I. Mutikainen, U. Turpeinen, J. Reedijk, Cryst. Growth Des. 7, 1669 (2007)
[27] T.J. Mooibroek, S.J. Teat, C. Massera, J. Reedijk, Cryst. Growth Des. 6, 1569 (2006)
[28] R.F.W. Bader, Chem. Rev. 91, 893 (1991)
[29] E. Cubero, M. Orozco, F.J. Luque, J. Phys. Chem. A 103, 315 (1999)
[30] I. Alkorta, F. Blanco, P.M. Deya, J. Elguero, C. Estarellas, A. Frontera, D. Quiñonero, Theor. Chem. Acc. 126, 1 (2010)
[31] F.J. Luque, M. Orozco, J. Comput. Chem. 19, 866 (1998)
[32] M.J. Frisch, G.W. Trucks, H.B. Schlegel, G.E. Scuseria, M.A. Robb, J.R. Cheeseman, J.A. Montgomery Jr., T. Vreven, K.N. Kudin, J.C. Burant, J.M. Millam, S.S. Iyengar, J. Tomasi, V. Barone, B. Mennucci, M. Cossi, G. Scalmani, N. Rega, G.A. Petersson, H. Nakatsuji, M. Hada, M. Ehara, K. Toyota, R. Fukuda, J. Hasegawa, M. Ishida, T. Nakajima, Y. Honda, O. Kitao, H. Nakai, M. Klene, X. Li, J.E. Knox, H.P. Hratchian, J.B. Cross, V. Bakken, C. Adamo, J. Jaramillo, R. Gomperts, R.E. Stratmann, O. Yazyev, A.J. Austin, R. Cammi, C. Pomelli, J.W. Ochterski, P.Y. Ayala, K. Morokuma, G.A. Voth, P. Salvador, J.J. Dannenberg, V.G. Zakrzewski, S. Dapprich, A.D. Daniels, M.C. Strain, O. Farkas, D.K. Malick, A.D. Rabuck, K. Raghavachari, J.B. Foresman, J.V. Ortiz, Q. Cui, A.G. Baboul, S. Clifford, J. Cioslowski, B.B. Stefanov, G. Liu, A. Liashenko, P. Piskorz, I. Komaromi, R.L. Martin, D.J. Fox, T. Keith, M.A. Al-Laham, C.Y. Peng, A. Nanayakkara, M. Challacombe, P.M.W. Gill, B. Johnson, W. Chen, M.W. Wong, C. Gonzalez, J.A. Pople, Gaussian-03 (Gaussian, Inc.: Wallingford, CT, 2003)
[33] S.B. Boys, F. Bernardy, Mol. Phys. 19, 553 (1970)
[34] F. Biegler-König, J. Schönbohm, D. Bayles, J. Comp. Chem. 22, 545 (2001)
[35] E. Sigfridson, U. Ryde, J. Comput. Chem. 19, 377 (1998)
[36] F.J. Luque, M. Orozco, MOPETE computer program (University of Barcelona, Barcelona,1998)
[37] B. Hernández, M. Orozco, F.J. Luque, J. Comput. Aided Mol. Des. 11, 153 (1997)
[38] F.J. Luque, M. Orozco, J. Chem. Soc., Perkin Trans. 2, 683 (1993)
[39] E. Scrocco, J. Tomasi, Top. Curr. Chem. 42, 95 (1973)
[40] M. Orozco, F.J. Luque, J. Comput. Chem. 14, 587 (1993)
[41] M.M. Francl, J. Phys. Chem. 89, 428 (1985)
[42] C. Garau, D. Quiñonero, A. Frontera, P. Ballester, A. Costa, P.M. Deya, Org. Lett. 5, 2227 (2003)
[43] E. Cubero, M. Orozco, F.J. Luque, J. Phys. Chem. A 103, 315 (1999)
[44] W. Zhu, X. Tan, J. Shen, X. Luo, F. Cheng, P.C. Mok, R. Ji, K. Chen, H. Jiang, J. Phys. Chem. A 107, 2296 (2003)
[45] C. Estarellas, A. Frontera, D. Quiñonero, I. Alkorta, P.M. Deyà, J. Elguero, J. Phys. Chem. A 113, 3266 (2009)
[46] F.H. Allen, Acta Crystallogr. B58, 380 (2002)
[47] A. Nangia, K. Biradha, G.R. Desiraju, J. Chem. Soc., Perkin Trans. 2, 943 (1996)
[48] J. Yang, B.R. Nelson, J.A. Weil, J.W. Quail, Act. Cryst. Section C 50, 1548 (1994)
[49] I.I Zviedre, E.M. Shvarts, V.K. Belskii, Zh. Neorg. Khim. 44, 1994 (1999)